M³⁺ Lanthanide Chloride Complexes in "Neutral" Room Temperature Ionic Liquids: A Theoretical Study

Alain Chaumont and Georges Wipff*

Laboratoire MSM, UMR CNRS 7551, Institut de Chimie, 4 rue B. Pascal, 67 000 Strasbourg, France

Received: July 30, 2003; In Final Form: December 16, 2003

The solvation of MCl_n^{3-n} lanthanide chloride salts (La^{3+}, Eu^{3+}, and Yb^{3+}; $n = 3$, 6, and 8) is studied by molecular dynamics simulations in two room-temperature ionic liquids which are "neutral" (Lewis acidity): [BMI][PF₆] composed of 1-butyl-3-methyl-imidazolium⁺,PF_6^- ions and [EMI][TCA] composed of 1-ethyl-3-methyl-imidazolium⁺,$AlCl_4^-$ ions. The simulations reveal the importance of the MCl_6^{3-} complex, commonly observed in solid-state structures and in chloride-containing solutions. This contrasts with the gas phase where, according to QM calculations, MCl_6^{3-} is unstable toward the dissociation of 1 to 2 Cl^- ions. In the two studied solvents, the MCl_n^{3-n} complexes with $n = 3$ to 6 remain bound during the simulation, while MCl_8^{5-} complexes lose two Cl^- anions and form MCl_6^{3-}. The only exception concerns $LaCl_8^{5-}$ which dissociates to $LaCl_7^{4-}$ in [EMI][TCA] solution. The first shell of MCl_3, MCl_4^-, and MCl_5^{2-} is mainly completed by solvent anions (about 3, 2, 1 PF_6^- and 4, 3, 1 $AlCl_4^-$ anions, respectively for M = Eu), while the three studied MCl_6^{3-} complexes are surrounded by a cage of 9−10 BMI⁺ or EMI⁺ cations, into which some solvent anions can be inserted. The results are important for our understanding of the solution state of trivalent actinide or lanthanide ions in room temperature ionic liquids.

Introduction

Room temperature ionic liquids, RTILs, based on alkyl-imidazolium cations (see Figure 1) exhibit interesting characteristics with respect to practical applications in many fields of chemistry and electrochemistry and are considered as a promising class of "green" solvents for a broad variety of weakly polar to polar solutes.[1−3] These ambient temperature molten salts have superior properties, as compared to organic solvents: low vapor pressure, high electrical conductivity and wide electrochemical windows, and nonflammability. Adequate selection of the solvent anion (hereafter noted Y^-) and/or the cation substituents allows to solubilize metallic ions or to extract them from an aqueous phase.[4−7] Recent publications also point to the growing interest in ionic liquids as new solvents for f-element separations[8−11] focusing, e.g., on uranyl complexation and solvation[12,13] or on the stabilization of unusual oxidation states of lanthanides.[14] RTILs may also be used to mimic solvation in high-temperature molten salts.[15] So far, little is known about microscopic details of the structure of RTILs and their solvation properties. Computer simulations may provide important insights into these issues, and a few reports appeared recently on the properties of liquid components,[16−20] on the structure of pure liquids,[21−24] and on the solutions of small neutral molecules.[25,26] We studied RTIL solutions of the uranyl and strontium salts,[27] as well as of the "naked" trivalent M³⁺ lanthanide cations whose first shell was found to consist of solvent anions only, with different coordination numbers, denticities, and dynamics features, depending on the solvent and lanthanide cation.[28]

The present paper focuses on RTIL solutions of lanthanide chloride complexes. Lanthanide halides are very common[29] and particularly relevant in RTILs that are prepared by mixing, e.g., ammonium or guanidinium chloride salts with $AlCl_3$, and the corresponding Cl^- over $AlCl_3$ ratio R allows to adjust the Lewis

Figure 1. Ionic components of imidazolium-based ionic liquids.

acidity of the solution.[30,31] At $R > 1$ the solution contains "free" Cl^- ions and is Lewis "basic", while at $R < 1$ it contains unsaturated chloride accepting species such as $Al_2Cl_7^-$ and is "acidic". In this paper, we consider a "neutral" liquid based on an equimolar mixture of 1-ethyl-3-methyl-imidazolium⁺,$AlCl_4^-$, hereafter noted [EMI][TCA], for which $R = 1$. The high affinity of TCA⁻ for water prevents such liquids to be used in liquid−liquid extraction of ions from aqueous phases. For that purpose, more hydrophobic anions such as PF_6^- or $(SO_2CF_3)_2N^-$ can be used.[32−34] This is why we decided to also simulate the lanthanide chloride complexes in [BMI][PF₆] solution, based on 1-butyl-3-methyl-imidazolium⁺,PF_6^- ions.

The studied solutes are the neutral MCl_3 and the negatively charged MCl_n^{3-n} species ($n = 4$, 5, 6, and 8). We want to investigate whether these complexes dissociate in the RTIL solution as they do in aqueous solution or remain stable, and to characterize their solvation: does MCl_3 behave as a neutral species with a similar "affinity" for the cationic and anionic solvent components, and is the solvation of the complexes with $n > 3$ determined by their negative charge? For the MCl_3, MCl_6^{3-} and MCl_8^{5-} systems, we compare the La^{3+}, Eu^{3+}, and Yb^{3+} cations of decreasing ionic radius (1.03, 0.95, and 0.87 Å, respectively),[35] while the tetra- and pentacoordinated chloride complexes are studied with Eu^{3+} only, for computer time saving purposes. As the PF_6^- and $AlCl_4^-$ anions can coordinate the metal in a monodentate or polydentate fashion, it will be
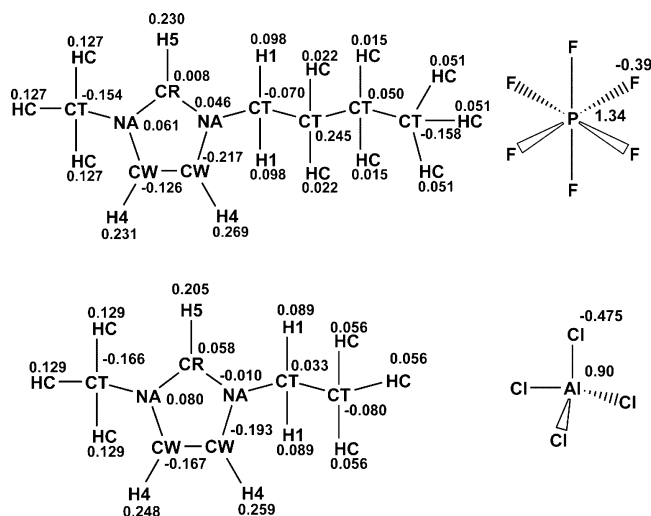
* Corresponding author. E-mail: wipff@chimie.u-strasbg.fr

Figure 2. AMBER atom types and charges used to simulate the [BMI]-[PF$_6$] and [EMI][TCA] ionic liquids.

interesting to compare these interactions as a function of the metal size. We assume that all species retain their integrity during the simulation, thus allowing neither for halide transfer reactions from the liquid to the cation, nor for halide elimination to form, e.g., Al$_2$Cl$_7^-$, Cl$^-$, or F$^-$ species. Another important question concerns the role of the surrounding medium on the properties of the first coordination shell of the lanthanide ions. The results in solution will thus be compared with those of MCl$_n^{3-n}$ complexes in the gas phase, as described by quantum mechanical calculations and by the force field models.

Methods

Molecular Dynamics Simulations. The systems were simulated by classical molecular dynamics (MD) using the modified AMBER 5.0 software[36] in which the potential energy U is described by a sum of bond, angle, and dihedral deformation energies and pairwise additive 1−6−12 (electrostatic and van der Waals) interactions between nonbonded atoms.

$$U = \sum_{\text{bonds}} k_b(b - b_0)^2 + \sum_{\text{angles}} k_\theta(\theta - \theta_0)^2 +$$

$$\sum_{\text{dihedrals}} \sum_n V_n[1 + \cos(n\varphi - \gamma)] +$$

$$\sum_{i<j} \frac{q_i q_j}{R_{ij}} - 2\epsilon_{ij}\left(\frac{R_{ij}^*}{R_{ij}}\right)^6 + \epsilon_{ij}\left(\frac{R_{ij}^*}{R_{ij}}\right)^{12}$$

Cross terms in van der Waals interactions were constructed using the Lorentz−Berthelot rules. The parameters used for the liquids have been tested on the pure liquid properties: those of EMI$^+$, BMI$^+$, and TCA$^-$ ions are taken from Andrade et al.,[22] while those of PF$_6^-$ anions are from ref 37 and have been used by Margulis et al. to simulate a RTIL.[38] The corresponding AMBER atom types and atomic charges are given in Figure 2. We note that for the gas-phase optimized BMI$^+$···PF$_6^-$ dimer, the AMBER interaction energy (−75.9 kcal/mol) is in excellent agreement with the BSSE corrected quantum mechanical calculated value (−76.2 kcal/mol; HF level with a 6-31G** basis set) and that both structures are similar.

The M^{3+} parameters ($R^*_{\text{La}} = 2.105$, $R^*_{\text{Eu}} = 1.852$, and $R^*_{\text{Yb}} = 1.656$ Å, $\epsilon_{\text{La}} = 0.06$, $\epsilon_{\text{Eu}} = 0.05$, and $\epsilon_{\text{Yb}} = 0.04$ kcal/mol) were fitted on free energies of hydration.[39] For Cl$^-$, we used the same van der Waals parameters as for the Cl(TCA) atoms

($R^* = 1.943$ Å, $\epsilon = 0.265$ kcal/mol),[22] for all chlorine atoms potentially coordinated to a given M^{3+} cation have the same size. Tests with a somewhat bigger anion (noted Cl$_{\text{hyd}}$; $R^* = 2.495$ Å, $\epsilon = 0.107$ kcal/mol) developed for free energies of hydration[40,41] were performed on the LaCl$_6^{3-}$ complex in solution. The 1−4 van der Waals interactions were scaled down by 2.0 and the 1−4 Coulombic interactions were scaled down by 1.2, as recommended by Cornell et al.[42] The pure liquids and solutions were simulated with 3D-periodic boundary conditions. Nonbonded interactions were calculated with a 12 Å residue based cutoff, correcting for the long-range electrostatics by using the Ewald summation method (PME approximation).[43,44] Tests on the [EMI][TCA] pure liquid using a larger cutoff (15 Å) showed that both cutoffs yield similar results and the shorter one was thus used to reduce the computational costs.

The MD simulations were performed at 300 K starting with random velocities. The temperature was monitored by coupling the system to a thermal bath using the Berendsen algorithm[45] with a relaxation time of 0.2 ps. All C−H bonds were constrained with SHAKE,[43,46] using the Verlet leapfrog algorithm with a time step of 2 fs to integrate the equations of motion.

We first equilibrated "cubic" boxes of pure liquids, containing 150 EMI$^+$ TCA$^-$ or 150 BMI$^+$ PF$_6^-$ ions, of 37.5 and 37.7 Å length, respectively, for the neutral solutions. After equilibration, the solvent densities (1.30 and 1.33 g/cm^3, respectively) were in fair agreement with experimental values (1.30[17,47] and 1.36 g/cm^3,[48] respectively) and the cation−anion radial distribution functions were similar to those published in refs 22 and 38 and with the neutron diffraction data of the [EMI][TCA] liquid.[49]

We then immersed one MCl$_n^{3-n}$ complex in the liquid, and total charge neutrality was achieved by removing n-3 PF$_6^-$ or TCA$^-$ solvent anions when $n > 3$. Equilibration started with 1500 steps of steepest descent energy minimization, followed by 50 ps of MD with fixed solutes ("BELLY" option of AMBER) at constant volume and by 25 ps at constant volume without constraints, followed by 25 ps at constant pressure of 1 atm. Then MD was run for 1.2 ns in the (N,V,T) ensemble. To check that the sampling is sufficient, we proceeded to mixing−demixing simulation tests. Solvent mixing (randomization) was obtained by 0.5 ns of MD in which the system was heated at 500 K and the electrostatics scaled down by a factor 100, keeping the solute frozen. This was followed by 0.75 ns of free MD at 300 K with reset electrostatics.

The MD trajectories were saved every 0.5 ps and analyzed with the MDS and DRAW software.[50] Typical snapshots were redrawn with VMD.[51] Insights into energy features were obtained by group component analysis, using a 17 Å cutoff distance and a reaction field correction for the electrostatics.[52] The average structure of the solvent around M^{3+} was characterized by the radial distribution functions (RDFs) of its anions (Al, Cl, P, F atoms) and cations (N$_{\text{ethyl}}$ atom of EMI$^+$ or N$_{\text{butyl}}$ atom of BMI$^+$) during the last 0.3 ns. The average coordination number (CN) of solvent anions or cations and its standard deviation are calculated up to a cutoff distance of the first peak of the RDF, as reported in the Tables.

Quantum Mechanics Calculations. The MCl$_n^{3-n}$ complexes ($n = 3$, 4, 5, and 6) were optimized without symmetry constraints by quantum mechanical calculations at the Hartree−Fock (HF) and DFT (B3LYP functional) levels of theory, using the Gaussian 98 software.[53] Optimizations on the larger complexes ($n = 8$) failed to converge.

As f orbitals do not play a major role in metal−ligand bonds,[54] the 46 core and 4f electrons of the lanthanides were
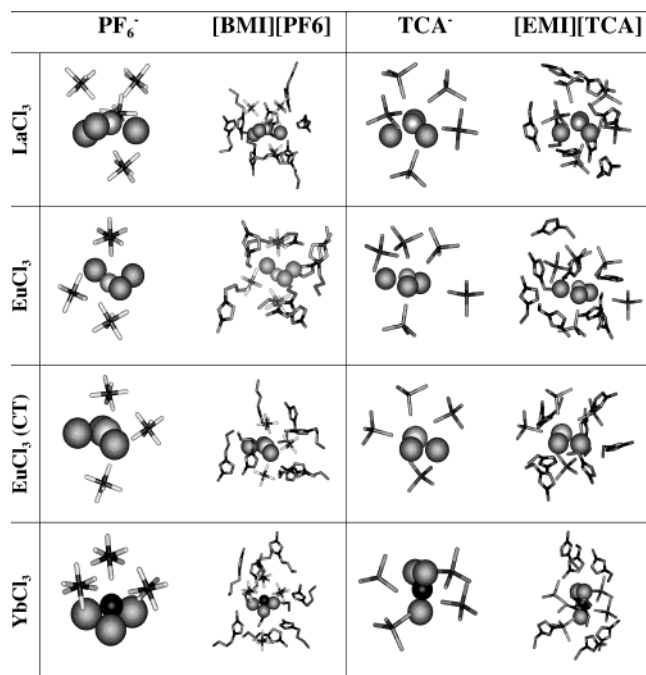
M^{3+} Lanthanide Chloride Salt Solvation

J. Phys. Chem. B, Vol. 108, No. 10, 2004 **3313**

Figure 3. MCl$_3$ complexes in [BMI][PF$_6$] (left) and [EMI][TCA] (right) ionic liquids. Final snapshots of the first solvation shell of anions only, and anions + cations. The radius is ≈8 Å, thus somewhat smaller than indicated by the BMI$^+$ or EMI$^+$ RDFs. A color version is given as Supporting Information (Figure S1).

described by quasi-relativistic effective core potentials (ECP) of the Stuttgart group.[55,56] For the valence orbitals, the affiliated (7s6p5d)/[5s4p3d] basis set was used, enhanced by an additional single f-function from ref 57. For the Cl atoms we compared the 6-31G* and 6-31+G* basis sets (HF and DFT calculations). The total energies of the MCl$_n^{3-n}$ complexes are given in Table S1 in the Supporting Information.

Results

The MCl$_n^{3-n}$ complexes (M = La, Eu, and Yb) were simulated with a purely noncovalent (van der Waals + Coulombic) model, thus allowing in principle for M–Cl bond dissociation. In the two liquids, however, all complexes remained bound until the end of the dynamics for n = 3 to 6. For n = 8, most of the species dissociated to MCl$_6^{3-}$ complexes. Generally, the first shell of MCl$_3$ is completed by solvent anions, whose number decreases as the M^{3+} lanthanide gets smaller (i.e., from La^{3+} to Yb^{3+}). It also decreases as the number of coordinated chloride anions increases and is generally smaller with PF$_6^-$ than with TCA$^-$ solvent anions. One also observes dynamic changes in solvent anion binding mode (monodentate/bidentate) and dynamics. Details are given below. The MCl$_n^{3-n}$ intracomplex "bonds" will be noted M–Cl, while the metal–halide intermolecular distances involving PF$_6^-$ or TCA$^-$ solvent anions will be noted M···F or M···Cl.

1. Solvation of the MCl$_3$ Complexes in [BMI][PF$_6$] and [EMI][TCA] Liquids. In the two liquids, all neutral MCl$_3$ complexes (M = La, Eu, and Yb) form a pseudo-D$_{3h}$ type arrangement, on the average. Schematically, the three Cl$^-$ anions sit in the "equatorial" plane, leaving room for additional apical coordination of $p+q$ solvent anions (p at one side and q at the other side of the equatorial plane). The average M-Cl bond distances are the same for a given cation in the two liquids and decrease with the cation size (2.66, 2.45, and 2.29 Å, respectively for La^{3+}, Eu^{3+}, and Yb^{3+}). Typical structures are shown in Figure 3 and solvent RDFs are given in Figure 4.
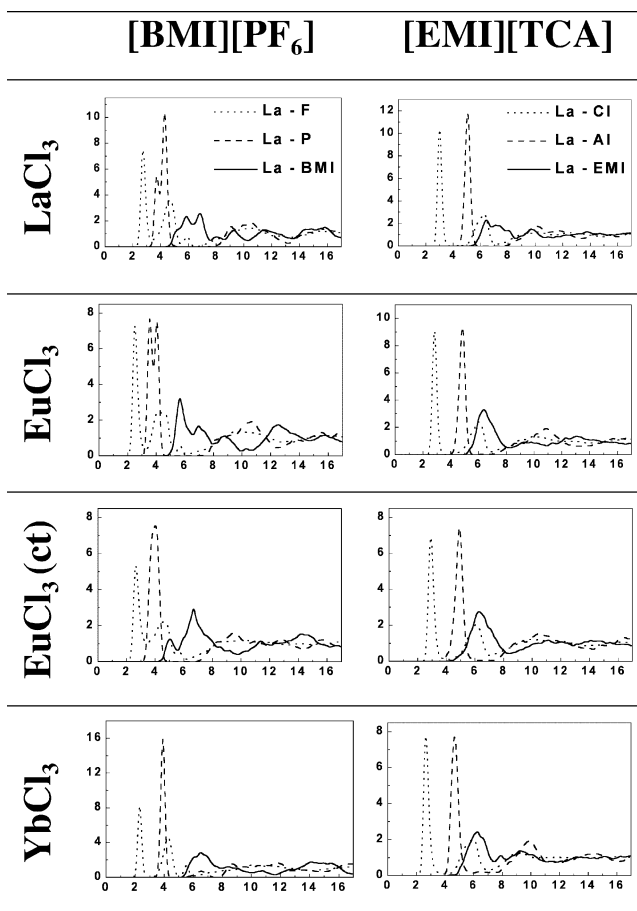

Figure 4. MCl$_3$ complexes in [BMI][PF$_6$] (left) and [EMI][TCA] (right) ionic liquids: radial distribution functions of the liquid around the M atom. Note the different scales of the graphs.

TABLE 1: Characteristics of the First Peak of the Solvent RDFs around M^{3+}: Coordination Number and RMS Fluctuations (first line), Distances (Å) of the First Maximum and Minimum (second line). Averages over the Last 0.3 ns of MD.

	[BMI][PF$_6$]			[EMI][TCA]		
	P	F	BMI	Al	Cl	EMI
LaCl$_3$	4.0 (0.0)	5.2 (0.5)	6.3 (0.5)	5.0 (0.0)	5.0 (0.0)	7.7 (0.7)
	3.8, 4.3; 5.4	2.8; 3.4	5.9, 6.9; 7.6	5.1; 6.0	3.0; 4.0	6.4; 8.6
EuCl$_3$	3.0 (0.0)	4.4 (0.5)	6.6 (0.6)	4.0 (0.0)	4.0 (0.1)	7.8 (0.8)
	3.6, 4.1; 4.8	2.5; 3.3	5.7, 7.0; 8.0	4.9; 6.3	2.9; 4.1	6.3; 8.3
EuCl$_3$(ct)	3.0 (0.0)	4.3 (0.8)	7.3 (0.6)	3.9 (0.3)	3.9 (0.4)	7.6 (0.6)
	4.0; 5.1	2.7; 3.4	6.7; 9.7	4.9; 5.7	2.8; 3.7	6.4; 8.4
YbCl$_3$	3.0 (0.0)	3.0 (0.0)	7.3 (0.7)	3.7 (0.5)	3.6 (0.5)	5.3 (0.7)
	3.9; 4.6	2.3; 2.9	6.5; 7.9	4.7; 5.9	2.7; 3.9	6.3; 7.5
EuCl$_4^-$	2.0 (0.0)	2.7 (0.5)	6.8 (0.7)	3.0 (0.2)	3.0 (0.2)	8.0 (0.5)
	3.6, 4.1; 4.8	2.5; 3.2	6.5; 7.5	4.9; 6.0	2.9; 3.9	6.0; 8.9
EuCl$_5^{2-}$	1.0 (0.0)	1.0 (0.1)	8.0 (0.2)	1.0 (0.0)	1.0 (0.0)	8.6 (0.6)
	4.1; 4.8	2.5; 3.2	5.6; 8.0	4.8; 5.7	2.8; 3.5	5.6; 8.9
LaCl$_6^{3-}$	a	a	10.0 (0.3)	a	a	10.0 (0.1)
	9.5; 12.5	9.4; 12.4	5.6; 9.6	9.1; 12.9	9.3; 12.2	5.8; 9.0
EuCl$_6^{3-}$	a	a	10.1 (0.3)	a	a	9.9 (0.5)
	8.5; 11.5	9.0; 12.8	5.4; 8.4	8.5; 11.9	9.4; 11.5	5.5; 9.0
EuCl$_6^{3-}$(ct)	a	a	10.1 (0.3)	a	a	10.5 (0.6)
	8.4; 12.7	9.0; 12.7	6.2; 8.6	8.8; 12.4	8.8; 11.0	5.4; 9.2
YbCl$_6^{3-}$	a	a	9.0 (0.0)	a	a	9.2 (0.4)
	9.0; 10.0	9.5; 12.8	5.7; 7.6	9.2; 12.1	9.9; 12.3	5.2; 8.5

^{a} Value not reported because this peak is ill-defined.

We first consider the [BMI][PF$_6$] solution. The M···solvent RDFs show that the first solvation shell of MCl$_3$ contains exclusively PF$_6^-$ anions (Figure 3) whose number and binding mode depend on M^{3+} (Table 1, Figure 4). Around LaCl$_3$, one

finds 1+3 PF_6^-, one being in the same plane as the three Cl^- anions (La···P distances are $\approx 3.8 \pm 0.2$ Å) and three being a little further away (La···P $\approx 4.1-4.3$ Å), on the other side. The equatorial PF_6^- anion is bidentate and the axial anions are generally monodentate but spin rapidly around their central P atom, leading to a total La^{3+} coordination of 5.2 ± 0.5 F atoms, on the average. For the smaller $EuCl_3$ and $YbCl_3$ complexes, only 3 PF_6^- complete the first solvation shell: 1 is equatorial, the other 1+1 ones are in apical positions. These complexes differ by the coordination mode of PF_6^-, however. The 3 PF_6^- anions around $YbCl_3$ adopt a fixed monodentate coordination (Yb···P distances ≈ 3.9 Å), while around $EuCl_3$ the equatorial and apical anions rapidly spin around their P atoms and exchange between monodentate and transient bidentate states. These two coordination modes around $EuCl_3$ lead to a splitting of the first peak of the RDFs to two sets of Eu···P distances, 3.5 Å for the equatorial (bidentate) PF_6^- and 4.0 Å for the apical (monodentate) ones. The first anion shell of MCl_3 complexes is surrounded and quasi-neutralized by a positively charged imidazolium "cage": the $LaCl_3$···BMI^+ RDF becomes nonzero after 4.3 Å and integrates to 6.3 ± 0.5 BMI^+ up to 7.6. We note that this second shell contains no solvent anion. The $EuCl_3$ and $YbCl_3$ complexes and their first shell PF_6^- anions are similarly surrounded by a "cage" of 6.6 and 7.3 BMI^+ cations, respectively. Around $YbCl_3$, one finds one PF_6^- anion inserted in this second shell.

In [EMI][TCA] solution, the first solvation shell of MCl_3 contains TCA^- anions only: 5.0 for $LaCl_3$, 4.0 for $EuCl_3$, and 3.7 for $YbCl_3$, on the average. $LaCl_3$ is coordinated to five Cl atoms stemming from the five monodentate TCA^- anions (one is equatorial, and the other 1+3 ones are apical). The average La···Al distance is $\approx 5.0-5.1$ Å, while the La···Cl_{TCA} distance is 3.0 Å $\pm$ 0.1. The solvation of $EuCl_3$ is similar, except that the equatorial TCA^- anion is missing, and the average Eu···Al and Eu···Cl distances are $\approx 0.1-0.2$ Å shorter. The first solvent shell of $YbCl_3$ is somewhat more complex to describe and more dynamic. During the first 1.1 ns, it contained 4 TCA^- anions (1 equatorial, and 1+2 in apical positions). After 1.1 ns one apical anion dissociated, leading to an octahedral halide arrangement around Yb^{3+}. To test the stability of this arrangement, we pushed the simulation for another 0.5 ns during which the dissociated TCA^- anion oscillated between coordinated ($\approx 20\%$) and uncoordinated states ($\approx 80\%$). In both states the coordinated TCA^- anions are monodentate, leading to a coordination number of 3.6 ± 0.5 Cl(TCA) atoms. The average Yb···Al and Yb···Cl distances are 4.7 Å and 2.7−2.8 Å, respectively.

The EMI^+ solvent cations sit beyond the first anionic shell, in a similar fashion for the three studied complexes. Their RDFs become nonzero after 5.0 Å and integrate to a total of 7.7 ± 0.7 (up to 8.6 Å) for $LaCl_3$, of 7.8 ± 0.8 (up to 8.6 Å) for $EuCl_3$ and 5.3 ± 0.7 EMI^+ cations (up to 7.5 Å) for $YbCl_3$.

We further decided to investigate the influence of halide to metal electron transfer on the solvation pattern of these complexes. To reduce CPU costs we limited the study to the $EuCl_3$ complex (hereafter noted $EuCl_3$(ct)) where the europium charge was reduced from +3 to +1.5 e and halide charges from −1.0 to −0.5 e. These values are close to Mulliken charges obtained by quantum mechanical calculations (see Tables 2 and S2).[58] We found no great differences between the solvation patterns of $EuCl_3$ vs $EuCl_3$(ct) complexes. Their RDF characteristics and their coordination numbers are very similar (Table 1). The most noticeable effect of charge reduction is the peak broadening in the Eu···TCA RDFs (Figure 4) as a result of

TABLE 2: QM Optimized Structures and Mulliken Charges of the MCl_n^{3-n} Complexes (DFT/6-31+G* calculations)[a]

	MCl_3	MCl_4^-	MCl_5^{2-}	MCl_6^{3-}
	M-Cl Distances (Å)			
La^{3+}	2.63 (D_{3h})	2.70 (T_d)	2.78/2.83 (C_{4v})	2.93 (O_h)
Eu^{3+}	2.57 (D_{3h})	2.60 (T_d)	2.69/2.74 (D_{3h})	2.83 (O_h)
Yb^{3+}	2.46 (D_{3h})	2.51 (T_d)	2.60/2.64 (D_{3h})	2.73 (O_h)
	Mulliken Charges on M atom			
La^{3+}	1.098	0.964	1.059	1.570
Eu^{3+}	0.862	0.732	0.834	1.548
Yb^{3+}	0.841	0.600	0.742	1.618

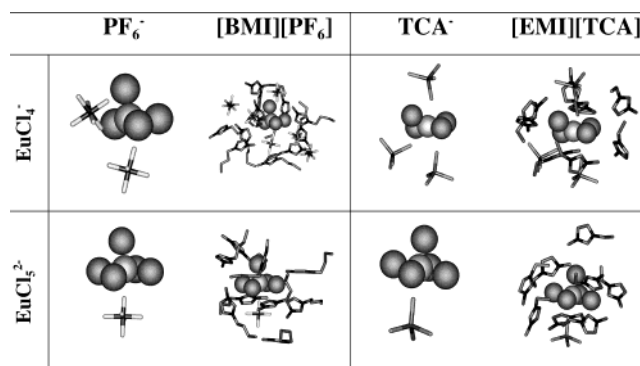[a] The results of DFT/6-31G*, HF/6-31G*, and HF/6-31+G* calculations are given in Table S2.

Figure 5. $EuCl_4^-$ and $EuCl_5^{2-}$ complexes in [BMI][PF$_6$] (left) and [EMI][TCA] (right) ionic liquids. Final snapshots of the first solvation shell of anions only, and anions + cations. A color version of the figure is given as Supporting Information (Figure S2).
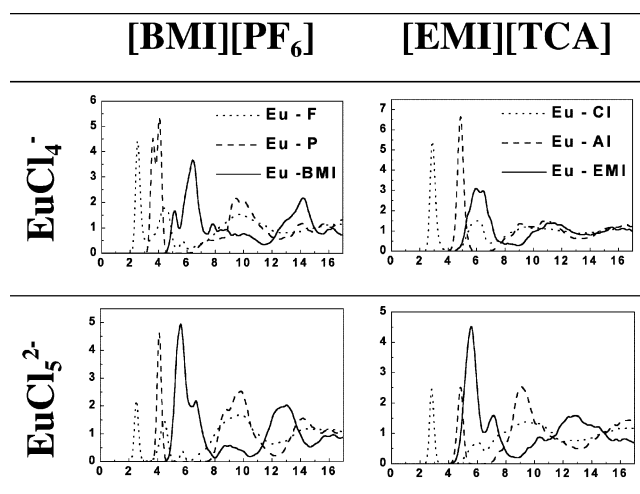

Figure 6. $EuCl_4^-$ and $EuCl_5^{2-}$ complexes in [BMI][PF$_6$] and [EMI]-[TCA] ionic liquids: radial distribution functions of the liquid around the Eu atom.

weakened electrostatic interactions which lead to longer distances and enhanced dynamics of the first shell anions.

2. Solvation of the $EuCl_4^-$ and $EuCl_5^{2-}$ Complexes in [BMI][PF$_6$] and [EMI][TCA] Liquids. The complexes with four and five chloride anions were simulated with Eu^{3+} only. The main results are shown in Figures 5 and 6. In the two liquids, the first shell of $EuCl_4^-$ contains a pseudo-tetrahedral arrangement of the Cl^- atoms, completed by 2.0 PF_6^- anions in [BMI][PF$_6$] solution or by 3.0 TCA^- anions in [EMI][TCA] solution. The PF_6^- anions exchange between monodentate and bidentate coordination, while the TCA^- anions bind monodentate, leading to total coordination numbers of 2.7 F atoms and 3.0 Cl(TCA) atoms, respectively, for europium.
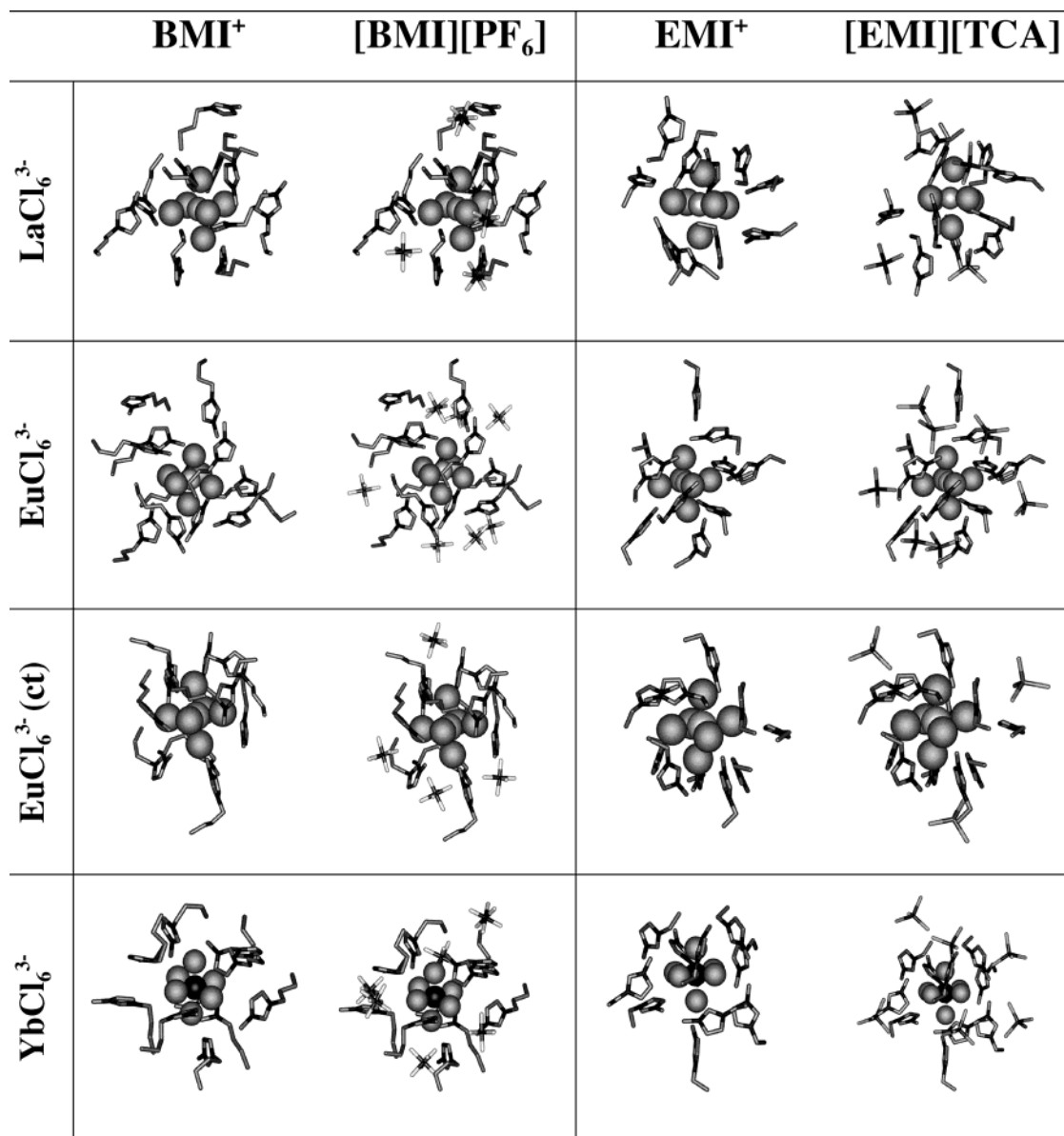
M³⁺ Lanthanide Chloride Salt Solvation

J. Phys. Chem. B, Vol. 108, No. 10, 2004 **3315**

Figure 7. MCl_6^{3-} complexes in [BMI][PF₆] and [EMI][TCA] ionic liquids. Final snapshots of the first solvation shell of anions only, and anions + cations. A color version of the figure is given as Supporting Information (Figure S3).

The chloride atoms of $EuCl_5^{2-}$ form a C_{4v} (4+1) arrangement, completed by 1.0 apically coordinated F(PF₆) or Cl(TCA) atom, which corresponds to octahedral arrangements of halides in the two solvents.

On the average, the Eu−Cl bond distances are similar in $EuCl_3$, $EuCl_4^-$, and $EuCl_5^{2-}$ complexes (≈2.8 Å), as are the shortest Eu···F and Eu···Cl contacts with the solvent molecules (≈2.5 and 2.8 Å, respectively). The second solvation shell of the $EuCl_4^-$ and $EuCl_5^{2-}$ complexes mostly contains imidazolium cations (≈7 and 8, respectively, in [BMI][PF₆] solution and ≈8 and 8.6, respectively, in [EMI][TCA] solution), at about 6 to 9 Å from the metal.

3. Solvation of the MCl_6^{3-} Complexes in [BMI][PF₆] and [EMI][TCA] Liquids. The Cl⁻ anions of the MCl_6^{3-} complexes are found to form an octahedron around the central cation (Figure 7). The average M−Cl distances (2.69 Å for La−Cl; 2.50 Å for Eu−Cl and 2.35 Å for Yb−Cl) are about 0.05 Å longer than in the corresponding MCl_3 complexes. The solvation patterns of the three complexes are similar in a given liquid (see Figures 7 and 8 and Table 1): they are surrounded by a positively charged cage formed by imidazolium cations at about

5.5 Å from M³⁺, comprising 10 cations around the lanthanum and europium complexes, and 9 cations around the smaller ytterbium one. Structures shown in Figure 7 and corresponding RDFs (Figure 8) show that there is no particular orientation of these imidazoliums which adopt tangential as well as perpendicular orientations with respect to MCl_6^{3-}.

In the two solvents, the RDFs around $YbCl_6^{3-}$ display well-separated peaks for the solvent cations and the solvent anions, which shows that the first solvation shell of this complex is exclusively formed by the cations. This is less the case for the $LaCl_6^{3-}$ and $EuCl_6^{3-}$ complexes whose cation and anion solvent RDFs somewhat overlap, indicating that solvent anions penetrate into the first shell: 7.5 ± 0.9 PF₆⁻ or 5.3 ± 1.4 TCA⁻ anions, and 3.3 ± 0.8 PF₆⁻ or 6.3 ± 1.4 TCA⁻ anions, respectively.

Given the report of the experimental diffusion coefficient D of $EuCl_6^{3-}$ in basic AlCl₃/EMI⁺Cl⁻ molten salts ($D = 2.50 \times 10^{-7}$ cm² s⁻¹ at 40 °C)[59] we calculated D for this complex in the [EMI][TCA] neutral liquid, using the Stokes−Einstein equation: $6Dt = \langle[r_i(t) - r_i(0)]^2\rangle$. The result ($D = 0.94 \times 10^{-7}$ cm² s⁻¹ at 25 °C; average over the last 0.3 ns) is in the right order of magnitude but smaller, as expected from the lower
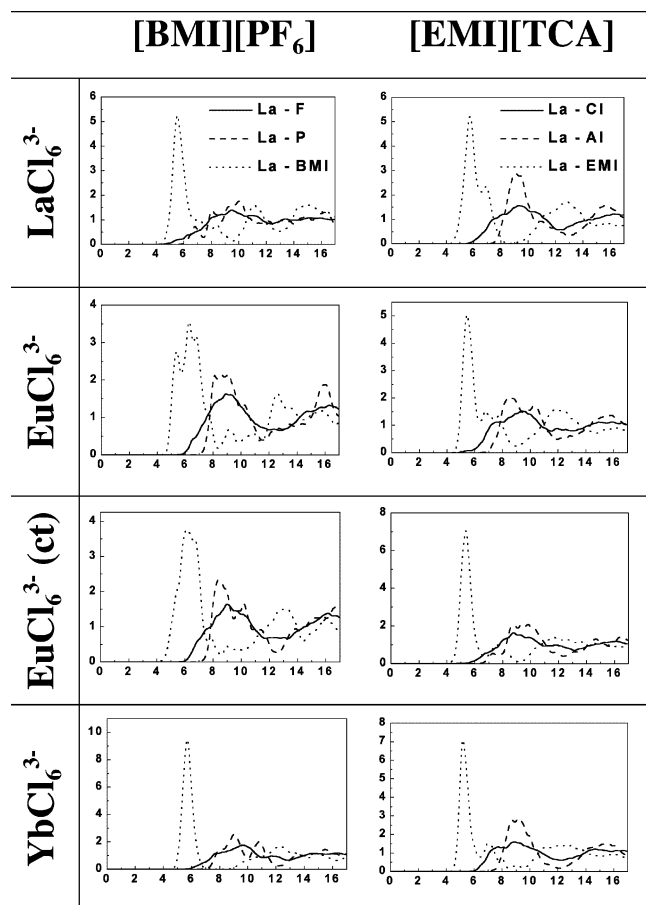
[BMI][PF$_6$]   [EMI][TCA]

Figure 8. MCl$_6^{3-}$ complexes in [BMI][PF$_6$] and [EMI][TCA] ionic liquids: radial distribution functions of the liquid around the M atom.

temperature. Note also that the experimental solution is basic, thus containing "free" Cl$^-$ solvent ions in excess, while the simulated solution contains AlCl$_4^-$ solvent anions only.

We also investigated the effect of "charge transfer" on the EuCl$_6^{3-}$ complex, which was simulated in the two liquids with reduced charges ($q_{Eu} = 1.5$ and $q_{Cl} = -0.75$ e) and noted EuCl$_6^{3-}$(ct). The simulations started with "random solvent", using the same protocol as with the original charges. In a given solvent, the solvent RDFs (Figure 8) and typical snapshots (Figure 7) are similar to the two sets of charges. The corresponding coordination numbers (Table 1) are also very similar. The only difference is the broadening of the first BMI$^+$ peak around EuCl$_6^{3-}$(ct) in the [BMI][PF$_6$] solution, indicating enhanced dynamics due to the reduced metal−chloride attractions.

4. Dissociation of the MCl$_8^{5-}$ Complexes in [BMI][PF$_6$] and [EMI][TCA] Liquids. As there are presently no experimental data on the status and stoichiometry of lanthanide chloride salts in the studied RTILs, we decided to also consider higher stoichiometries, in which the metal is close to saturation. We thus studied the more negatively charged MCl$_8^{5-}$ complexes in which the metal is octa-coordinated. According to simulations in [EMI][TCA] solution, the naked M^{3+} ions[28] are surrounded by eight TCA$^-$ anions which might, via a least pathway motion, lead to the MCl$_8^{3-}$ complexes, and we wanted to investigate whether such complexes remain stable in solution. Their starting structure was thus extracted from the M(TCA)$_8^{5-}$ complexes in which TCA$^-$ were replaced by Cl$^-$ anions.

In [BMI][PF$_6$] solution, the three studied MCl$_8^{5-}$ species decomposed into a MCl$_6^{3-}$ complex and two Cl$^-$ anions which sit in the second solvation shell, at about 7.5−8.5 Å from the central metal. The solvation patterns are analogous to those

described above, i.e., a positively charged cage of imidazolium cations around MCl$_6^{3-}$, into which the two chlorides are inserted. In [EMI][TCA] solution, YbCl$_8^{5-}$ and EuCl$_8^{5-}$ also dissociated to MCl$_6^{3-}$, plus two Cl$^-$ anions at 7.5−8.5 Å. In the case of LaCl$_8^{5-}$, only one Cl$^-$ decomplexed. In the resulting LaCl$_7^{4-}$ complex, the chlorides form a 4+1+2 pattern around La^{3+}, 4 being in the equatorial plane, and 1+2 in apical positions. The decomplexed Cl$^-$ anion sits at the end of the simulation at about 8.5 Å from the La atom.

Several tests were performed in [EMI][TCA] solution to see to which extent the seven coordination of lanthanum was model dependent. As too large coordination numbers may result from too small ligands, we decided to increase the size of Cl$^-$ and to take the parameters derived from hydration energies,[39] instead of the Cl(TCA) ones. With this "big" Cl$_{hyd}$ model and the original one, we simulated the LaCl$_9^{6-}$ complex, whose structure was extracted from the simulation of La^{3+} where one TCA$^-$ is bidentate.[28] With the two Cl$^-$ models, the complex dissociated to LaCl$_7^{4-}$ as did LaCl$_8^{5-}$, confirming the coordination of seven chlorides to the metal. The two chloride models were also tested on the LaCl$_6^{3-}$ complex. The resulting La−Cl distances (2.69 and 3.0 Å, respectively, with the Cl(TCA) and Cl$_{hyd}$ models) bracket the distance of 2.79 Å observed in the solid-state structure of a LaCl$_6$(imidazolium)$_3$ salt.[60] This suggests that the seven chloride coordination of lanthanum in [EMI][TCA] is unlikely to be due to unreasonable sizes of the metal and of the halides, but is stabilized by the solvent.

5. Insights into Energy Features of Solvation. The average interaction energies E_{SL} between a given MCl$_n^{3-n}$ solute S and a liquid L reveal interesting evolutions, as a function of the number n of halides and the liquid components. First, all E_{SL} energies are negative, indicating stabilizing interactions with the solvents. We consider the europium complexes first and, in the two studied liquids, the largest E_{SL} values are found for the most charged EuCl$_6^{3-}$ solute (≈ -570 kcal/mol), while the smallest E_{SL} corresponds to EuCl$_3$ neutral (≈ -150 kcal/mol in the two solvents). Comparatively, changes in E_{SL} energies from one lanthanide cation to the other, or from one solvent to the other, are much smaller (less than 60 and 30 kcal/mol, respectively). Splitting E_{SL} into the cationic E_{SL}^+ (imidazolium cations) and anionic E_{SL}^- (PF$_6^-$ or TCA$^-$ anions) contributions shows contrasted effects. For the MCl$_3$ solutes, E_{SL}^+ and E_{SL}^- are both negative, and E_{SL}^- is of somewhat larger magnitude than E_{SL}^+, in keeping with the first-shell anionic solvent interactions described above. This contrasts with the MCl$_6^{3-}$ complexes, for which E_{SL}^+ is highly attractive (≈ -1820 to -1920 kcal/mol), while E_{SL}^- is repulsive (≈ 1290 to 1320 kcal/mol), and similar values are obtained in the two solvents. This reflects the solvation features described above.

For the EuCl$_4^-$ and EuCl$_5^{2-}$ complexes, attractive interactions with the solvent also stem from the imidazolium cations ($E_{SL}^+ \approx -610$ to -1200 kcal/mol), while the PF$_6^-$ or TCA$^-$ contributions are repulsive ($E_{SL}^- \approx 450$ to 900 kcal/mol), due to the repulsion of these anions with the chlorides. E_{SL} increases in magnitude with the number of halide atoms, i.e., from ≈ -150 kcal/mol for MCl$_3$ to ≈ -300 kcal/mol for EuCl$_5^{2-}$ in the two solvents.

Finally, comparing lanthanides of different size gives no regular trend, due to different contributions of the solvent cations and anions. The lanthanum complex is best solvated in the MCl$_3$ series, but is the least well solvated in the MCl$_6^{3-}$ series, as found for the "naked" M^{3+} cations.[28]

Discussion and Conclusion

We report a molecular dynamics investigation of the solvation of neutral and negatively charged lanthanide halides in two neutral RTILs as a function of the number of coordinated halides. The noncovalent interactions are represented by 1−6−12 potentials, thus assuming that these interactions are mainly steric and electrostatic in nature and determined by cation−anion coulombic interactions with local steric effects influencing the final orientation, as suggested from the analysis of the solid-state structure of RTIL analogues.[61] This does not mean that charge transfer, polarization, and many-body effects are negligible, especially as far as interactions with naked M³⁺ ions are concerned. In the studied systems, however, the lanthanides are neutralized by counterions, and their polarizing effect should be less important. We also notice that the 1−6−12 parameters used for the lanthanide cations allow to depict their main hydration features (free energies of hydration, average coordination numbers, and distances).[39] As reported in the original references[22,38] and in our previous studies,[27,28] the parameters used for the solvents also account for their main properties (density, average structure) and nicely fit the interaction energy and geometry of the BMI⁺ PF₆⁻ dimer, as compared to the quantum mechanical optimized one. We thus feel that the results are reasonable. Furthermore, the similarity between the solvation patterns of the EuCl₃ and the EuCl₆³⁻ complexes obtained in the two liquids without charge transfer (q_{Eu} = 3.0 e) as well as with charge transfer (q_{Eu} = 1.5 e) confirms that the solvation in the studied RTILs is not critically dependent on the choice of the electrostatic representation of the solutes, at least as far as structural features are concerned.

Another methodological issue concerns the sampling of the relevant states of the RTIL molecules. We believe that the simulations are long enough for the solvent molecules to diffuse and properly solvate the lanthanide complexes. This is further confirmed by mixing−demixing simulations we performed on the EuCl₃ and EuCl₄⁻ complexes in [BMI][PF₆] solution, after which the RDFs were quasi-identical to the original ones, as well as by sampling tests we performed with the M³⁺ cations in the two liquids.[28]

We report a detailed analysis of the interactions between the ionic components of two studied RTILs and the MCl_n^{3-n} lanthanide complexes, as a function of n. Solvation is determined by the strong tendency of the metal to saturate its first coordination shell with anions. The first shell of MCl₃, MCl₄⁻, and MCl₅²⁻ is indeed mainly completed by solvent anions (about 3, 2, 1 PF₆⁻ and 4, 3, 1 AlCl₄⁻ anions, respectively for M = Eu). In the three studied MCl₆³⁻ complexes, the metal is shielded from solvent by the chloride octahedral cage, and these complexes are surrounded by a cage of 9−10 imidazolium cations, into which some solvent anions penetrate when M = La or Eu. Minor differences are found from one lanthanide ion to the other. As expected, the M−Cl and M···Y⁻ distances shorten, and the anions become more monodentate as the lanthanide cation gets smaller.

An important issue concerns the nature of the MCl_n^{3-n} halides: what is the best n in a given solvent, and what is the role of the solvent on n? First insights come from comparison with the gas phase, where the stepwise addition of Cl⁻ anions was studied by QM for n = 3 to 6. The starting structures were extracted from the MD trajectories and were optimized without symmetry constraints. Thus, some MCl₃ complexes are D_{3h}, others are C_{3v}, but these forms are close in energy (they differ by less than 1 kcal/mol).[62−64] The same occurs with MCl₅²⁻ complexes, which may be D_{3h} or C_{4v}. For LaCl₅²⁻, the C_{4v}
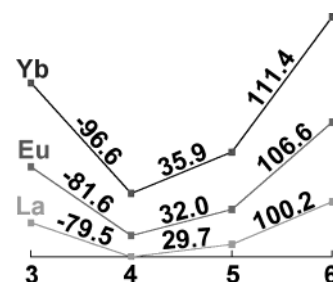

Figure 9. QM calculated (DFT-B3LYP/ 6-31+G* level) energy changes (kcal/mol) as a function of n for the reaction $MCl_n^{3-n} + Cl^- = MCl_{n+1}^{2-n}$. The results obtained at the HF and DFT levels with the 6-31G* and 6-31+G* basis sets are given in Figure S4. The corresponding gas-phase MD calculated energies obtained with different models are given in Figure 10.

form is less stable than the D_{3d} one by 1.2 kcal/mol only at the DFT/6-31+G* level. The optimized distances and Mulliken charges[58] are given in Tables 2 and S2 (Supporting Information). The halide binding energies have been calculated according to eq 1:

$$MCl_n^{3-n} + Cl^- = MCl_{n+1}^{2-n} \qquad (1)$$

They are presented in a graphical form in Figures 9 (BSSE corrected[65] DFT/6-31+G* results) and S1 (DFT/6-31G*, HF/6-31G* and HF/6-31*G* results). All methods yield similar trends for the three lanthanide cations, indicating that Cl⁻ addition to MCl₃ is favorable, while the MCl₅²⁻ and MCl₆³⁻ complexes are unstable with respect to the dissociation toward smaller complexes (by 30−36 kcal/mol and 100−111 kcal/mol, respectively, at the DFT/6-31+G* level for lanthanum−ytterbium complexes).

Similar trends are obtained when the complexes are simulated with the empirical force field methods. We compared their relative stabilities after 500 ps of dynamics in the gas phase at 300 K using two charge distributions (3.0 vs 1.5 e on Europium and Cl charges adjusted accordingly) and with two Cl models (the "big" Cl_hyd versus the "smaller" Cl_TCA). The results (see Figure 10) obtained with the four models confirm an energy stabilization from 3 to 4 or 5 coordination and an energy destabilization from 4 or 5 to 6 chlorides.[65] The most noticeable difference between QM and MD results is an inversion for the 4 versus 5 complexes with the Eu(3.0) model, which is of limited consequence, however, given that in solution both complexes are less stable than the 6-coordinated complex. Also note the satisfactory agreement between QM and force field methods, which confirms that the relative stabilities of the halide complexes are dominated by the electrostatic + van der Waals interactions. The most important result here is that the observation of MCl₆³⁻ species in condensed phases does not result from their intrinsic stability, but rather from stabilizing interactions with the solvent (see Table 3). For instance, when going from EuCl₅²⁻ to EuCl₆³⁻ complexes, the solvation energy increases by ≈270 kcal/mol, which overcompensates the loss of internal stabilities (about 110 kcal/mol with the QM method and 94 to 133 kcal/mol with the force field method).

On the computational side, we notice that all studied complexes with up to six chlorides remain bound in the two solutions. This contrasts with the dissociation of the larger MCl₈⁵⁻ complexes, which form MCl₆³⁻ species (the only exception being LaCl₇⁴⁻ in [EMI][TCA] solution). Simulations of naked M³⁺ lanthanides in basic solutions in which Cl⁻ anions

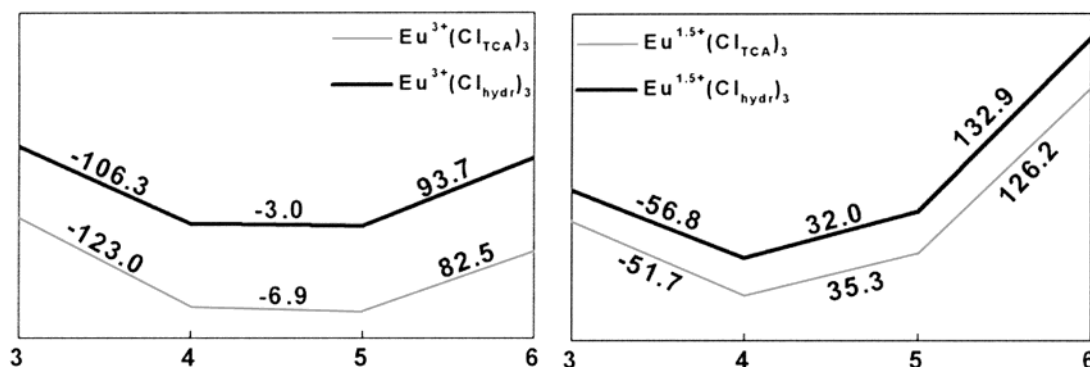**3318** *J. Phys. Chem. B, Vol. 108, No. 10, 2004*

Chaumont and Wipff

Figure 10. Relative energies (kcal/mol) of the $EuCl_3$, $EuCl_4^-$, $EuCl_5^{2-}$ and $EuCl_6^{3-}$ complexes obtained by MD simulations in the gas phase with two different charge distributions ($q_{Eu} = 3.0$ versus $q_{Eu} = 1.5$ e and Cl charges adjusted accordingly) and two Cl models (Cl_{TCA} versus Cl_{hydr}).

TABLE 3: Average Interaction Energies and RMS Fluctuations (kcal/mol) between the MCl_n^{3-n} Complexes and the Ionic Components (BMI$^+$ or EMI$^+$ Cations and PF$_6^-$ or TCA$^-$ Anions) of the Solvents

	[BMI][PF$_6$]			[EMI][TCA]		
	[BMI]	[PF$_6$]	[BMI][PF$_6$]	[EMI]	[TCA]	[EMI][TCA]
LaCl$_3$	−73 (6)	−126 (11)	−199 (15)	−79 (5)	−101 (7)	−180 (10)
EuCl$_3$	−54 (5)	−96 (6)	−150 (8)	−61 (5)	−82 (6)	−143 (8)
YbCl$_3$	−45 (4)	−129 (8)	−175 (9)	−57 (4)	−86 (9)	−143 (10)
EuCl$_4^-$	−617 (7)	448 (9)	−169 (11)	−609 (9)	453 (10)	−156 (9)
EuCl$_5^{2-}$	−1195 (13)	897 (12)	−298 (12)	−1213 (18)	908 (15)	−305 (15)
LaCl$_6^{3-}$	−1823 (17)	1304 (17)	−518 (14)	−1861 (24)	1313 (22)	−548 (16)
EuCl$_6^{3-}$	−1861 (18)	1288 (16)	−572 (14)	−1889 (25)	1317 (25)	−572 (16)
YbCl$_6^{3-}$	−1895 (16)	1316 (16)	−583 (15)	−1906 (19)	1312 (19)	−594 (15)

are in large excess also lead to the spontaneous formation of MCl_6^{3-} complexes.[66] The status of the Cl$^-$ anions thus likely depends on their concentration and on the composition of the RTIL.

There are a number of experimental results that hint at the importance of the MCl_6^{3-} motive in ionic environments. MX_6^{3-} octahedra (X = F, Cl, Br) have been characterized by Raman spectroscopy in high-temperature melt mixtures of MY_3−AX salts (M is a lanthanide cation, A is an alkali cation and X, Y are halide anions).[67−69] MCl_6^{3-} is also found in the solid-state structures of $LaCl_6(imidazolium)_3$,[60] $MCl_6(dimethylammonium)_3$ (with M = Er or Tm)[70] and $YbCl_6(methylammonium)_3$.[71] The $CeCl_6^{3-}$, $EuCl_6^{3-}$, and $NdCl_6^{3-}$ complexes have been characterized by electrochemical and spectroscopic studies in basic molten melts.[72,73] It has also been noted that the solubility of lanthanide chloride salts in $BMI^+Cl^-/AlCl_3$ mixtures increases with the basicity of the liquid.[74] According to electrochemical studies in $EMI^+Cl^-/AlCl_3$ molten salts, Eu(III) and Eu(II) are better solvated in basic than in acidic melts.[59] All these data and the affinity of smaller halide complexes for halogenated solvent anions found in our study point to the importance of the MCl_6^{3-} complex. As concerns the lanthanum case, our finding of $LaCl_7^{4-}$ stability in the [EMI][TCA] solution is consistent with the simulation results of Hutchinson et al. on LaCl$_3$ melts.[75] Using a more elaborate polarizable potential model, the authors conclude that the lanthanum cation is seven to eight coordinated. Coming to real ionic liquid solutions, it is also stressed that, in addition to the solvent basicity/acidity balance, impurities may determine the nature and solvation of the lanthanide complexes. We hope that the reported theoretical results will stimulate further experimental and theoretical studies.

Supporting Information Available: Tables and color figures of the structures and complexes described herein. This material is available free of charge via the Internet at http://pubs.acs.org.

References and Notes

(1) Welton, T. *Chem. Rev.* **1999**, *99*, 2071−2083.

(2) Hagiwara, R.; Ito, Y. *Fluorine Chem.* **2000**, *105*, 221.

(3) Wasserscheid, P.; Keim, W. *Angew. Chem., Int. Ed.* **2000**, *39*, 3772−3789.

(4) Dai, S.; Ju, Y. H.; Barnes, C. E. *J. Chem. Soc., Dalton Trans.* **1999**, 1201−1202.

(5) Visser, A. E.; Swatlosli, R. P.; Reichert, W. M.; Griffin, S. T.; Rogers, R. D. *Ind. Eng. Chem. Res.* **2000**, *39*, 3596−3604.

(6) Dietz, M. L.; Dzielawa, J. A. *Chem. Commun.* **2001**, 2124−2125.

(7) Chun, S.; Dzyuba, S. V.; Bartsch, R. A. *Anal. Chem.* **2001**, *73*, 3737−3741.

(8) Costa, D. A.; Smith, W. H.; Dewey, H. J. In *Molten Salts XII*; Trulove, P. C., DeLong, H. C., Stafford, G. R., Deki, S., Eds.; The Electrochemical Society Proceedings Series: Pennington, NJ, 2000; pp 1820−1825.

(9) Bradley, A. E.; Hatter, J. E.; Nieuwenhuyzen, M.; Pitner, W. R.; Seddon, K. R.; Thied, R. C. *Inorg. Chem.* **2002**, *41*, 1692−1694.

(10) Visser, A. E.; Rogers, R. D. *J. Solid State Chem.* **2003**, *171*, 106−113.

(11) Jensen, M. P.; Neuenfeind, J.; Beitz, J. V.; Skanthakumar, S.; Sonderholm, L. *J. Am. Chem. Soc.* **2003**, *125*, 15466−15473, and references therein.

(12) Hopkins, T. A.; Berg, J. M.; Costa, D.; Smith, W.; Dewey, H. J. *Inorg. Chem.* **2001**, *40*, 1820−1825.

(13) Visser, A. E.; Jensen, M. P.; Laszak, I.; Nash, K. L.; Choppin, G.; Rogers, R. D. *Inorg. Chem.* **2003**, *42*, 2197−2199.

(14) Billard, I.; Moutiers, G.; Labet, A.; ElAzzi, A.; Gaillard, C.; Mariet, C.; Lutzenkirchen, K. *Inorg. Chem.* **2003**, *42*, 1726−1733.

(15) Dai, S.; Toth, L. M.; DelCul, G. G.; Metcalf, D. H. *J. Phys. Chem.* **1996**, *100*, 220−223.

(16) Dymek, C. J. J.; Stewart, J. J. P. *Inorg. Chem.* **1989**, *28*, 1472.

(17) Takahashi, S.; Suzuya, K.; Kohara, S.; Koura, N.; Curtiss, L. A.; Saboungi, M. L. *Zeit. Physik. Chem.* **1999**, *209*, 209−211.

(18) Sitze, M. S.; Schreiter, E. R.; Patterson, E. V.; Freeman, R. G. *Inorg. Chem.* **2001**, *40*, 2298−2304.

(19) Meng, Z.; Dolle, A.; Carper, W. R. *J. Mol. Struct. (THEOCHEM)* **2002**, *585*, 119−128.

M^{3+} Lanthanide Chloride Salt Solvation

J. Phys. Chem. B, Vol. 108, No. 10, 2004 **3319**

(20) Turner, E. A.; Pye, C. C.; Singer, R. D. *J. Phys. Chem. A* **2003**, *107*, 2277−2288.

(21) Hanke, C. G.; Price, S. L.; Lynden-Bell, R. M. *Mol. Phys.* **2001**, *99*, 801−809.

(22) Andrade, J. D.; Böes, E. S.; Stassen, H. *J. Phys. Chem. B* **2002**, *106*, 13344−13351.

(23) Shah, J. K.; Brennecke, J. F.; Maginn, E. J. *Green Chemistry* **2002**, *4*, 112−118.

(24) Morrow, T. I.; Maginn, E. J. *J. Phys. Chem. B* **2002**, *106*, 12807−12813.

(25) Hanke, C. G.; Atamas, N. A.; Lynden-Bell, R. M. *Green Chemistry* **2002**, *4*, 107−111.

(26) Hanke, C. G.; Johansson, A.; Harper, J. B.; Lynden-Bell, R. M. *Chem. Phys. Lett.* **2003**, *374*, 85−90.

(27) Chaumont, A.; Engler, E.; Wipff, G. *Inorg. Chem.* **2003**, *42*, 5348−5356.

(28) Chaumont, A.; Wipff, G. *Phys. Chem. Chem. Phys.* **2003**, *5*, 3481−3488.

(29) *Halides of the lanthanides and actinides*; Brown, Ed.; Wiley−Interscience: New York, 1968.

(30) Hussey, C. L. *Adv. Molten Salt Chem.* **1983**, *5*, 185−230.

(31) Chum, H. L.; Osteryoung, R. A. In *Ionic Liquids*; Inman, D., Lovering, D. G., Eds.; Plenum: New York, 1981; p 407.

(32) Huddleston, J. G.; Willauer, H. D.; Swatloski, R. P.; Visser, A. E.; Rogers, R. D. *Chem. Commun.* **1998**, 1765−1766.

(33) Visser, A. E.; Swatloski, R. P.; Griffin, S. T.; Hartman, D. H.; Rogers, R. D. *Sep. Sci. Technol.* **2001**, *36*, 785−804.

(34) Gutowski, K. E.; Broker, G. A.; Willauer, H. D.; Huddleston, J. G.; Swatloski, R. P.; Holbrey, J. D.; Rogers, R. D. *J. Am. Chem. Soc.* **2003**, *125*, 6632−6633.

(35) *The Chemistry of the Actinide Elements*; Katz, J. J., Seaborg, G. T., Morss, L. R., Eds.; Chapman and Hall: London, 1986.

(36) Case, D. A.; Pearlman, D. A.; Caldwell, J. C.; Cheatham, T. E., III; Ross, W. S.; Simmerling, C. L.; Darden, T. A.; Merz, K. M.; Stanton, R. V.; Cheng, A. L.; Vincent, J. J.; Crowley, M.; Ferguson, D. M.; Radmer, R. J.; Seibel, G. L.; Singh, U. C.; Weiner, P. K.; Kollman, P. A. AMBER 5, University of California, San Francisco, 1997.

(37) Kaminski, G. A.; Jorgensen, W. L. *J. Chem. Soc., Perkin Trans. 2* **1999**, *2*, 2365−2375.

(38) Margulis, C. J.; Stern, H. A.; Berne, B. J. *J. Phys. Chem. B* **2002**, *106*, 12017−12021.

(39) van Veggel, F. C. J. M.; Reinhoudt, D. *Chem. Eur. J.* **1999**, *5*, 90−95.

(40) Berny, F. Thesis, 2000, Université Louis Pasteur, Strasbourg.

(41) Jost, P.; Schurhammer, R.; Wipff, G. *Chem. Eur. J.* **2000**, *23*, 4255−4264.

(42) Cornell, W. D.; Cieplak, P.; Bayly, C. I.; Gould, I. R.; Merz, K. M.; Ferguson, D. M.; Spellmeyer, D. C.; Fox, T.; Caldwell, J. W.; Kollman, P. A. *J. Am. Chem. Soc.* **1995**, *117*, 5179−5197.

(43) Allen, M. P.; Tildesley, D. J. In *Computer Simulation of Liquids*; van Gunsteren, W. F., Weiner, P. K., Eds.; Clarendon Press: Oxford, 1987.

(44) Essmann, U.; Perera, L.; Berkowitz, M. L. *J. Chem. Phys.* **1995**, *103*(19), 8577−8593.

(45) Berendsen, H. J. C.; Postma, J. P. M.; van Gunsteren, W. F.; DiNola, A. *J. Chem. Phys.* **1984**, *81*, 3684−3690.

(46) Ryckaert, J. P.; Ciccotti, G.; Berendsen, H. J. C. *J. Comput. Phys.* **1977**, *23*, 327−336.

(47) Fannin, A. A.; Floreani, D. A.; King, L. A.; Landers, J. S.; Piersma, B. J.; Stech, D. J.; Vaughn, R. L.; Wilkes, J. S.; L., W. J. *J. Phys. Chem.* **1984**, *88*, 2614.

(48) Gu, Z.; Brennecke, J. F. *J. Chem. Eng. Data* **2002**, *47*, 339.

(49) Takahashi, S.; Suzuka, K.; Kohara, S.; Koura, N.; Curtiss, L. A.; Saboungi, M. L. *Z. Phys. Chem.* **1999**, *209*, 209.

(50) Engler, E.; Wipff, G., unpublished.

(51) Humphrey, W.; Dalke, A.; Schulten, K. *J. Mol. Graph.* **1996**, *14*, 33−38.

(52) Tironi, I. G.; Sperb, R.; Smith, P. E.; van Gunsteren, W. F. *J. Chem. Phys.* **1995**, *102*, 5451−5459.

(53) Frisch, M. J.; Trucks, G. W.; Schlegel, H. B.; Scuseria, G. E.; Robb, M. A.; Cheeseman, J. R.; Zakrzewski, V. G.; Montgomery, J. A., Jr.; Stratmann, R. E.; Burant, J. C.; Dapprich, S.; Millam, J. M.; Daniels, A. D.; Kudin, K. N.; Strain, M. C.; Farkas, O.; Tomasi, J.; Barone, V.; Cossi, M.; Cammi, R.; Mennucci, B.; Pomelli, C.; Adamo, C.; Clifford, S.; Ochterski, J.; Petersson, G. A.; Ayala, P. Y.; Cui, Q.; Morokuma, K.; Malick, D. K.; Rabuck, A. D.; Raghavachari, K.; Foresman, J. B.; Cioslowski, J.; Ortiz, J. V.; Stefanov, B. B.; Liu, G.; Liashenko, A.; Piskorz, P.; Komaromi, I.; Gomperts, R.; Martin, R. L.; Fox, D. J.; Keith, T.; Al-Laham, M. A.; Peng, C. Y.; Nanayakkara, A.; Gonzalez, C.; Challacombe, M.; Gill, P. M. W.; Johnson, B.; Chen, W.; Wong, M. W.; Andres, J. L.; Gonzalez, C.; Head-Gordon, M.; Replogle, E. S.; Pople, J. A. *Gaussian 98*, Revision A.5; Gaussian, Inc.: Pittsburgh, PA, 1998.

(54) Maron, L.; Eisenstein, O. *J. Phys. Chem. A* **2000**, *104*, 7140−7143.

(55) Dolg, M.; Stoll, H.; Savin, A.; Preuss, H. *Theor. Chim. Acta* **1989**, *75*, 173−194.

(56) Dolg, M.; Stoll, H.; Savin, A.; Preuss, H. *Theor. Chim. Acta* **1993**, *85*, 441−450.

(57) Ehlers, A. W.; Böhme, M.; Dapprich, S.; Gobbi, A.; Höllwarth, A.; Jonas, V.; Köhler, K. F.; Stegmann, R.; Veldkamp, A.; Frenking, G. *Chem. Phys. Lett.* **1993**, *208*, 111.

(58) We prefer Mulliken charges over the ESP ones, because the former a priori reflect the electron reorganization (mainly charge transfer and polarization) better than ESP charges do in such complexes, due to the possible biased contribution of hidden atoms in the ESP procedure. However, both procedures were compared in the EuCl$_6^{3-}$ complex and were found to yield similar europium charges: the Mulliken charge is +1.54 e while the ESP charge is +1.82 e or +1.69 e, depending on the choice of the Europium radius (1.5 and 2.0 Å, respectively); HF calculation with the 6-31G* basis set and Merz−Kollman fitting procedure.

(59) Gau, W. J.; Sun, I. W. *J. Electrochem. Soc.* **1996**, *143*, 914−919.

(60) Matsumoto, K.; Tsuda, T.; Nohira, T.; Hagiwara, R.; Ito, Y.; Tamada, O. *Acta Crystallogr. Sect. C − Cryst. Struct. Comm.* **2002**, *C58*, m186−m187.

(61) Fuller, J.; Carlin, R. T.; Long, H. C. D.; Haworth, D. *J. Chem. Soc., Chem. Commun.* **1994**, 299−300.

(62) Adamo, C.; Maldivi, P. *J. Phys. Chem. A* **1998**, *102*, 6812−6820.

(63) Adamo, C.; Maldivi, P. *Chem. Phys. Lett.* **1997**, *268*, 61−68.

(64) Molnar, J.; Hargittai, M. *J. Phys. Chem.* **1995**, *99*, 10780−10784.

(65) Boys, S. F.; Bernardi, F. *Mol. Phys.* **1970**, *19*, 553−566.

(66) Chaumont, A. Thesis, University of Strasbourg, in preparation.

(67) Dracopoulos, V.; Gilbert, B.; Borrensen, B.; Photiadis, G. M.; Papatheodorou, G. N. *J. Chem. Soc., Faraday Trans.* **1997**, *93*, 3081−3088.

(68) Photiadis, G. M.; Borresen, B.; Papatheodorou, G. N. *J. Chem. Soc., Faraday Trans.* **1998**, *94*, 2605−2613.

(69) Dracopoulos, V.; Gilbert, B.; Papatheodorou, G. N. *J. Chem. Soc., Faraday Trans.* **1998**, *94*, 2601−2604.

(70) Becker, A.; Urland, W. *J. Alloys Compd.* **1998**, *275*, 62.

(71) Czjek, M.; Fuess, H.; Pabst, I. *Z. Anorg. Allg. Chem.* **1992**, *617*, 105.

(72) Lin, F. M.; Hussey, C. L. *J. Electrochem. Soc.* **1993**, *140*, 3093−3096.

(73) Lipsztajn, M.; Osteryoung, R. A. *Inorg. Chem.* **1985**, *24*, 716−719.

(74) Bourg, S.; Dalbies, A.; Lacquement, J. *PRACTIS* conference, 2003.

(75) Hutchinson, F.; Rowley, A. J.; Walters, M. K.; Wilson, M.; Madden, P. A. *J. Chem. Phys.* **1999**, *111*, 2028−2037.